

Title

Efficacy of chitinase-3-like protein 1 as an *in vivo* bone formation predictable marker of maxillary/mandibular bone marrow stromal cells

Naohiro Komabashiri, Fumio Suehiro, Masakazu Ishii, Masahiro Nishimura

Department of Oral and Maxillofacial Prosthodontics, Kagoshima University Graduate School of Medical and Dental Science, 8-35-1 Sakuragaoka, Kagoshima 890-8544, Japan

Corresponding author

Fumio Suehiro

Department of Oral and Maxillofacial Prosthodontics, Kagoshima University Graduate School of Medical and Dental Science, 8-35-1 Sakuragaoka, Kagoshima 890-8544, Japan

E-mail: fsuehiro@dent.kagoshima-u.ac.jp

Abstract

Introduction: Maxillary/mandibular bone marrow stromal cells (MBMSCs) are a useful cell source for bone regeneration in the oral and maxillofacial region. To further ensure the clinical application of MBMSCs in bone regenerative therapy, it is important to determine the bone formation capacity of

MBMSCs before transplantation. The aim of this study is to identify the molecular marker that determines the *in vivo* bone formation capacity of MBMSCs.

Methods: The cell growth, cell surface antigens, *in vitro* and *in vivo* bone formation capacity of MBMSCs were examined. The amount of chitinase-3-like protein 1 (CHI3L1) secreted into the conditioned medium was quantified. The effects of CHI3L1 on the cell growth and osteogenic differentiation potential of MBMSCs and on the cell growth and migration of vascular endothelial cells and fibroblasts were examined.

Results: The cell growth, and *in vitro* and *in vivo* bone formation capacity of the cells treated with different conditions were observed. MBMSCs that secreted a large amount of CHI3L1 into the conditioned medium tended to have low *in vivo* bone formation capacity, whereas MBMSCs that secreted a small amount of CHI3L1 had greater *in vivo* bone formation capacity. CHI3L1 promoted the migration of vascular endothelial cells, and the cell growth and migration of fibroblasts.

Conclusion: Our study indicates that the *in vitro* osteogenic differentiation capacity of MBMSCs and the *in vivo* bone formation capacities of MBMSCs were not necessarily correlated. The transplantation of high CHI3L1 secretory MBMSCs may suppress bone formation by inducing fibrosis at the site. These results suggest that the CHI3L1 secretion levels from MBMSCs may be used as a predictable marker of bone formation capacity *in vivo*.

Highlights

- In vitro and in vivo bone formation capacities of MBMSCs were not correlated.
- MBMSCs with high CHI3L1 secretion tended to have low *in vivo* bone formation.
- MBMSCs with low CHI3L1 secretion tended to have high *in vivo* bone formation.
- CHI3L1 can be *in vivo* bone formation capacity predictable marker of MBMSCs.

Key words

jaw bone marrow stromal cells, bone formation capacity, Chitinase-3-like protein 1, migration

Abbreviations

MSCs: mesenchymal stem cells

MBMSC: maxillary/mandibular bone marrow stromal cells

CHI3L1: chitinase-3-like protein 1

α -MEM: alpha modified Eagle's minimum essential medium

FBS: fetal bovine serum

ALP: Alkaline phosphatase

β -TCP: beta-tricalcium phosphate

HUVEC: human umbilical vein endothelial cells

NHDF: normal human dermal fibroblasts

BMSC: bone marrow-derived stem cell

Main Text

1. Introduction

Autologous bone grafting is the gold standard for reconstructing severe bone defects; however, the method is limited by the quantity of bone that can be collected and potential paresthesia of donor sites [1].

Therefore, an innovative treatment method with less donor burden is required to reconstruct severe bone defects.

Mesenchymal stem cells (MSCs) proliferate in an undifferentiated state and differentiate into bone, cartilage, tendon, muscle, and adipose tissue [2-5]. Various bone regeneration studies using MSCs derived from the iliac crest have been reported [6, 7]. While isolation and expansion of MSCs from the iliac crest have been standardized, the collection of MSCs from the iliac crest is not common for dentists. Compared with iliac crest MSCs, the collection of maxillary/mandibular bone marrow stromal cells (MBMSCs) from the jaw bone marrow does not require a major surgical procedure, especially for dentists. MBMSCs and iliac MSCs have comparable osteogenic differentiation potential; however, MBMSCs have a weaker potential to differentiate to chondrocytes and adipocytes because of their different stem properties [8, 9]. MBMSCs have been a candidate cell source for bone regenerative medicine in the maxillofacial region [10], and several bone regeneration studies using MBMSCs have been reported [11, 12]. The population of plating bone marrow cells is heterogeneous; some MBMSCs have progenitor properties and multi-potent differentiation capacity, whereas others are devoid of this capacity [13]. Therefore, to use

MBMSCs for bone regeneration therapy, it is necessary to determine their capacity to form bone *in vivo* at an early culture stage.

Various methods are used to measure the osteogenic differentiation potential of MSCs, such as alizarin red staining, ALP activity quantification, and gene expression level measurements of RUNX2, Osterix, and osteopontin [14, 15]. Conversely, mRNA levels of osteogenic markers or various cell surface marker expressions *in vitro* are not predictable for the *in vivo* bone formation capacity of iliac MSCs [16]. Cell sorting of iliac bone marrow stromal cells or adipose tissue-derived stromal cells using flow cytometry can collect MSCs with high osteogenic differentiation potential [17, 18]. However, the number of colony forming stromal cells collected from jaw bone marrow is small and it is difficult to isolate high bone-forming capacity cells by cell sorting in clinical settings. In addition, cell culture for cell transplantation therapy is expensive; therefore, it is necessary to find a simple marker to determine the high bone-forming capacity of cells *in vivo* at an early stage of culture.

MSCs secrete various factors that influence osteogenesis, angiogenesis, and cell migration in auto or paracrine manners [19, 20]. In addition, MSC conditioned medium promotes high bone formation *in vivo* [21]. We hypothesized that the *in vivo* bone formation capacity of MBMSCs for transplantation could be predicted in advance by quantifying the factors secreted by MBMSCs into culture supernatant. The purpose of this study is to identify *in vivo* bone formation predictor markers released in MBMSC culture conditioned medium.

2. Methods

2.1. Human MBMSC culture from maxillary/mandibular bone marrow

Human bone marrow was collected from maxillary/mandibular bone according to a protocol approved by the ethical committee at Kagoshima University. Bone marrow aspirates were collected as previously reported [22]. Briefly, all samples were collected noninvasively using a GC biopsy needle (GC, Tokyo, Japan) and syringe via a hole drilled in the maxilla or mandible during dental implant surgery. Collected bone marrow aspirates (approximately 150 μ l) were immediately suspended with 80 μ l Heparin Sodium Injection (5,000units/5-ml, MOCHIDA PHARMACEUTICAL CO LTD, Tokyo, Japan). A portion of the collected bone aspirate was analyzed using an automated hematology analyzer (MEK-6358, Nihon Kohden, Tokyo, Japan), and the white blood cell number and white/red blood cell ratio (W/R ratio) was counted. Bone marrow aspirates from seven donors were seeded at a density of approximately 5×10^4 white blood cells/cm² on tissue culture plates and the proliferated cells were used as MBMSCs. The medium was alpha modified Eagle's minimum essential medium (α -MEM; Thermo Fisher Scientific, Waltham, MA, USA) containing 10% fetal bovine serum (FBS) and 1% antibiotic–antimycotic (Thermo Fisher Scientific) (growth medium). MBMSCs were incubated at 37°C in a humidified incubator and 5% CO₂/95% air atmosphere for 5–7 days with careful handling until cells adhered to the plate. The adhered MBMSCs were fed with fresh growth medium every 3 days. Cell passaging was performed prior to

confluence. MBMSCs were suspended with trypsin and EDTA (0.25%: Thermo Fisher Scientific) and seeded at a density of 5×10^3 cells/cm² on 100 mm tissue culture dishes (Corning, NY, USA) in 10 ml of growth medium. MBMSCs obtained from the third to fifth passages were used for the following experiments.

Cell growth was examined using a cumulative cell growth curve. MBMSCs were seeded at a density of 5×10^3 cells/cm² on 12-well tissue culture dishes and maintained in 1 ml of growth medium until confluent. Just before approaching confluence, MBMSCs were suspended with trypsin and EDTA and counted. The remaining cells were reseeded at a density of 5×10^3 cells/cm² for the next passage. This process was continued until the MBMSCs growth stopped.

2.2. Cell growth analysis

Human umbilical vein endothelial cells (Lonza, Basel, Switzerland) (HUVECs) were cultured in endothelial cell basal medium-2 (Lonza), supplemented with EGM-2MV BulletKit (Lonza). Normal human dermal fibroblasts (NHDFs, Lonza) and MBMSCs were cultured in growth medium. Each cell was seeded in a 96-well plate at 1,000 cells/well and cultured with their growth medium for 6 hours and the medium was changed to include CHI3L1 (0.01, 0.1, 1, 10, or 100 ng/ml). Seventy-two hours later, Premix WST-1 Cell Proliferation Assay System (Takara Bio Inc., Shiga, Japan) was added at 10 μ L/well and incubated at 37°C for 40 minutes. The absorbance of the solution at 450 nm was measured using a

spectrophotometric microplate reader (Multiskan FC; Thermo Fisher Scientific).

2.3. Flow cytometric analysis

MBMSCs were analyzed by flow cytometry to detect cell surface antigens previously reported as criteria for identifying MSCs [23]. MBMSCs were harvested with trypsin and EDTA, centrifuged at $1,500 \times g$ for five minutes, and resuspended at 1×10^4 cells/ml in PBS containing 0.5% bovine serum albumin, 2 mM EDTA, and FcR Blocking Reagent (Miltenyi Biotec, Bergisch Gladbach, Germany). Aliquots were then incubated with individual antibodies: anti-human CD73 (phycoerythrin (PE)-conjugated mouse IgG1; BioLegend, San Diego, CA, USA), anti-human CD90 (fluorescein isothiocyanate (FITC)-conjugated mouse IgG1; BioLegend), anti-human CD105 (FITC-conjugated mouse IgG1; Ansell Corp., Bayport, MN, USA), anti-human CD14 (FITC-conjugated mouse IgG1; BioLegend), anti-human CD34 (PE-conjugated mouse IgG1; BioLegend), and anti-human CD45 (FITC-conjugated mouse IgG1; BioLegend). FITC-conjugated mouse IgG1 (BioLegend), and PE-conjugated mouse IgG1 (BioLegend) were the isotype controls. Flow cytometric analysis was performed with Guava easyCyte 5 (Merck, Darmstadt, Germany), and data analysis was performed using Guava Express Pro (Merck).

2.4. Osteogenic differentiation

MBMSCs were seeded at a density of 5×10^3 cells/cm² in 24-well tissue culture dishes and were fed

growth medium until confluent. The MBMSCs were maintained in osteogenic induction medium (α -MEM supplemented with 10% FBS, 0.1 μ M Dexamethasone, 50 μ g/ml L-Ascorbic acid 2-phosphate, and 10 mM β -Glycerophosphate). MBMSCs were fed osteogenic induction medium every 2–3 days.

2.5. Alkaline phosphatase (ALP) activity assay

Osteogenic differentiated MBMSCs were washed twice with physiological saline, then 0.2% Triton-X100 was added to the culture well and MBMSCs were disrupted on ice for 10 seconds using a Q55 Sonicator (Qsonica, Newtown, CT, USA). Lysed MBMSCs were centrifuged at 12,000 \times g for 5 min. The supernatant was incubated with 16 mM PNPP (SIGMA FAST *p*-nitrophenyl phosphate tablet sets; Merck), for 10–30 min at 37°C, and the reaction was stopped by the addition of 1 N NaOH. The absorbance of the solution at 405 nm was measured using a spectrophotometric microplate reader. The ALP activity was normalized against the amount of protein in the same well and the value was expressed as ALP activity per minute per milligram protein.

2.6. Alizarin red staining

Osteogenic differentiated MBMSCs were washed twice with a solution containing 10 mM Tris-HCl, pH 7.6, and 0.9% NaCl and then fixed in 95% ethanol at room temperature for 1 hour. MBMSCs were stained with 1% Alizarin-red S (Merck) for 10 minutes at room temperature.

2.7. Experimental animals and transplantation of MBMSCs

The animal selection, management, and surgical procedure were approved by the animal experiment ethics committee of Kagoshima University (Approval Number D20013). Twenty-one, 4-week-old male C.B-17 immunodeficient mice (KBT Oriental., LTD, Saga, Japan) (SCID mice) were used in this experiment. MBMSCs from 7 samples were transplanted into three mice (N=3). The mice were anesthetized with a combination of inhalation anesthesia with isoflurane (1%–2%) and intraperitoneal injection of xylocaine (0.2%, 0.1 ml). After anesthesia, the animals were cleansed with povidone iodine. After an approximately 1 cm skin incision, muscle dissection, and periosteal elevation, the parietal bone was carefully exposed. The graft was then implanted under the parietal periosteum and the skin and periosteum were sutured with absorbable thread. During surgery, xylocaine (2%, 0.1 ml) was administered locally to relieve postoperative pain. In addition, 6 mg/kg of gentamicin was administered intraperitoneally to prevent postoperative infection. After 8 weeks, the mice were euthanized and the transplant site was collected for histological observation.

Graft materials were prepared as follows. Each solution of 5×10^5 MBMSCs was mixed with 25 mg β -tricalcium phosphate (β -TCP) (Olympus Terumo Biomaterials Corp., Tokyo, Japan). After incubation at 37°C for 60 minutes, the mixture was centrifuged at $35 \times g$ for 1 minute and the supernatant was discarded. The pellet of β -TCP with adhered cells was mixed with 3% atelocollagen (KOKEN CO., LTD,

Tokyo Japan) and incubated at 37°C for 30 minutes for gel formation. These mixtures were transplanted under the periosteum of the parietal bone of the immunodeficient mice (KBT Oriental., LTD, Saga, Japan).

2.8. Histological examination and histometric analysis

Eight weeks after transplantation, mice were euthanized by cervical dislocation after anesthetization with isoflurane. The transplanted site of parietal bone was collected and the soft tissue was removed and fixed in 4% paraformaldehyde for 24 hours at 4°C. Tissue was treated with 25% formalin formate demineralization solution for 1 day, dehydrated with 70% ethanol, and embedded in low-melting-point paraffin. The samples were cut into 5 µm sections with a rotating microtome. Sections were subjected to hematoxylin-eosin and Masson's trichrome staining. Immunohistological analysis for angiogenesis was performed with CD31 immunostaining (DAB, Anti-CD31(ab182981): abcam, Cambridge, UK). The *in vivo* bone formation capacity was expressed as the percentage of bone area per tissue area (BA/TA) in each visual field of transplanted region, excluding the recipient bone and β-TCP. BA/TA was measured using Image-J (National Institutes of Health, Bethesda, MD, USA) and the results are represented by the means ± SD from three different sections of the same sample.

Angiogenesis at the transplanted site was expressed as the number of running blood vessels per unit area, excluding the recipient bone and β-TCP. The number of running vessels was counted in three randomly

chosen fields from each section and the mean \pm SD was calculated.

2.9. Antibody array of the culture supernatant

MBMSCs were seeded at a density of 5×10^3 cells/cm² on 100 mm tissue culture dishes and maintained in growth medium until confluent. The growth medium was changed to serum-free medium (α -MEM supplemented with 1% antibiotic–antimycotic) and cultured for 24 hours. The MBMSC culture supernatant was collected, and subjected to a Proteome Profiler Human Angiogenesis Array Kit (R&D Systems, Minneapolis, MN, USA), Human Chemokine Array Kit (R&D Systems), and Human XL Cytokine Array Kit (R&D Systems), according to the manufacturer's protocols.

2.10. Quantification of the secreted protein

The above culture supernatant were assessed by a Human Chitinase 3-like 1 (CHI3L1) Quantikine ELISA Kit (R&D Systems), Human CXCL1/GRO alpha Quantikine ELISA Kit (R&D Systems), Human CCL2/MCP-1 Quantikine ELISA Kit (R&D Systems), Human CCL7/MCP-3 Quantikine ELISA Kit (R&D Systems), and Human IL-8/CXCL8 Quantikine ELISA Kit (R&D Systems) following the manufacturer's protocols. The absorbance of the solution at 450 nm and 570 nm was measured using a spectrophotometric microplate reader and the readings at 570 nm were subtracted from the readings at 450 nm. Because the number of cells in each MBMSC at the time of confluence was different, the secretion amount of each factor was normalized per 1×10^4 cells.

2.11. RNA isolation and real-time reverse transcription polymerase chain reaction

MBMSCs were seeded at a density of 5×10^3 cells/cm² on 100 mm tissue culture dishes and maintained in growth medium until confluent. Total RNA was isolated with ISOGEN (NIPPON GENE, Tokyo, Japan). Reverse transcription was performed using ReverTra Ace qRCR RT Master Mix (TOYOBO, Osaka, Japan) (mixed Oligo dT Primer and Random Primer) following the manufacturer's protocol. Quantitative real-time PCR was performed using the CFX Connect Real-Time System (Bio-Rad, Hercules, CA, USA) and the THUNDERBIRD SYBR Green PCR kit (Toyobo). The sequences of all the primers used are shown in Table 1. The expression level of each mRNA was normalized to the expression level of GAPDH.

2.12. Cell migration assay

Cell migration assays were performed using Transwell 24-well tissue culture plates made of polycarbonate membranes (Corning) with 8 μ m pores. MBMSC, HUVECs, and NHDFs were seeded in the inner chamber of the transwell plate at a concentration of 1×10^5 cells/100 μ L. The inner chambers were placed in an outer chamber filled with 800 μ L of each growth medium containing CHI3L1 (0.01–100 ng/mL) and the chambers were incubated at 37°C for 6 hours. Cells migrating to the outer surface of the membrane were fixed in 4% paraformaldehyde and then cold methanol and stained using the May–

Giemsa method. The number of migrated cells in each sample was counted in five randomly selected fields at a magnification of 10 \times .

2.13. Statistical analysis

Data are expressed as the mean \pm standard deviation. Statistical analysis was performed using IBM SPSS Statistics Version 26. Comparison between two groups was performed using Student's t-tests. Statistical analysis for multiple comparisons among groups was performed using one-way ANOVA, and the Tukey post hoc correction was applied.

3. Results

3.1. Characterization of MBMSCs

Maxillary/mandibular bone marrow samples were obtained from seven donors and the cell growth capacity, *in vitro* osteogenic differentiation potential, and expression profiles of cell surface markers were evaluated. There was inter-sample variation in cell proliferating capacity, and all samples proliferated to at least 1×10^7 cells in 60 days of culture (Figure 1A). ALP activity indicating the early stage of osteogenic differentiation were measured 7 days after osteogenic induction, and alizarin red staining indicating the calcification of the cell layer occurred 14 days after osteogenic induction. MBMSC1, 2, 3, and 4 showed high ALP activity and MBMSC1, 2, 3, 4, and 6 showed obvious calcium deposition (Figure 1B and C). In the flow cytometric analysis, all MBMSCs showed cell surface antigen expression profiles similar to those previously reported as MSCs (positive for CD73, CD90, and CD105 and negative for CD14, CD34, and CD45) (Table 2).

3.2. Bone formation capacity of MBMSCs

MBMSCs and β -TCP/collagen mixtures were transplanted under the periosteum of the parietal bone of immunodeficient mice and 8 weeks later, the transplant site was collected and histologically analyzed. Newly formed bone was observed continuously from recipient bone; however, the amount of formed bone varied among each MBMSC transplanted group (Figure 2A). As a result, MBMSCs were divided

into a high bone formation group (MBMSC3, 4, 5, 7) and a low bone formation group (MBMSC1, 2, 6) (Figure 2B).

3.3 Relationship between protein secretion and gene expression level of MBMSCs *in vitro* with bone formation capacity *in vivo*

Comprehensive protein analysis was performed using the conditioned medium from MBMSC 3, 4, 5 (high bone formation group) and MBMSC6 (low bone formation group). Analysis using three different antibody array kits showed that CHI3L1, GRO α , MCP-1, MCP-3, and IL-8 measurements differed between the two MBMSC groups with different bone formation capacity. All these protein amounts were less in the MBMSCs group with high bone formation capacity and more in the MBMSC group with low bone formation capacity (Figure 3). The amount of specific protein in the MBMSC conditioned medium was then quantified by ELISA. The amount of secreted CHI3L1 was high in MBMSC1, 2, 6 and low in MBMSC3, 4, 5, 7, which indicates that the MBMSC group with high bone formation capacity secreted less CHI3L1, and the MBMSC group with low bone formation capacity secreted more CHI3L1 in the culture stage (Figure 4A). Table 3 shows the amount of CHI3L1 secreted from MBMSCs during culture and the BA/TA ratio. Among the other four proteins tested (GRO α , MCP-1, MCP-3, and IL-8), no correlation between the secreted protein amount and the bone formation capacity was observed (Figure 4B–E). Similarly, CHI3L1 mRNA expression was negatively correlated with bone forming potential

(Figure 5A), while the other gene expressions did not show any correlation (Figure 5B–E).

3.4 Effects of CHI3L1 on the cell growth and osteogenic differentiation of MBMSCs

To examine the effect of CHI3L1 on MBMSC growth, cells were incubated with different concentrations of CHI3L1 (0.01–100 ng/ml) for 72 hours. Treatment with CHI3L1 did not affect the MBMSC growth (Figure 6A). To examine the effect of CHI3L1 on the osteogenic differentiation capacity of MBMSCs, ALP activity assay and alizarin red staining were performed. In all MBMSCs, there were no difference in the ALP activity and the degree of calcification regardless of the CHI3L1 concentration (Figure 6B and C).

3.5 Effects of CHI3L1 on cell growth and cell migration of other cells

Cell growth assays of HUVECs and NHDFs were performed to determine the paracrine effect of secreted CHI3L1 from transplanted MBMSC to surrounding recipient cells. Treatment with CHI3L1 for 72 hours showed no significant difference in HUVEC cell growth at any concentration. Alternatively, treatment with 1–100 ng/ml CHI3L1 significantly promoted NHDFs growth (Figure 7A).

A migration assay was performed to evaluate the migration effect by CHI3L1 on HUVECs and NHDFs. The quantitative analysis showed that CHI3L1 significantly promoted HUVECs migration, peaking at 0.1 ng/ml (Figure 7B and C). The migration effect of CHI3L1 was observed on NHDFs in a dose dependent

manner (Figure 7D and E). The migration effect by CHI3L1 was not observed in the MBMSCs at any experimental dose (data not shown).

3.6 Histological analysis at the transplantation site

The transplant sites of collagen fibers were evaluated using Masson's trichrome staining. The low bone formation groups (MBMSC1 and 6) showed strong collagen fiber staining near the recipient bone (Figure 8A) and the high bone formation group (MBMSC3 and 5) was less fibrotic (bone and β -TCP are slightly blue) (Figure 8A). Immunohistochemical analysis was performed using CD31 antibody to observe angiogenesis. The MBMSC1 transplanted site had significantly more running vessels stained with CD31 than the MBMSC3 and five transplanted sites (Figure 8B and C). These results show that fibrosis and angiogenesis occurred actively at the site where MBMSCs releasing high concentrations of CHI3L1 were transplanted.

4. Discussion

In this study, the *in vivo* bone formation capacity of MBMSCs was inconsistent with the results of *in vitro* MBMSCs osteogenic differentiation. Alternatively, since the CHI3L1 secretion pattern from MBMSCs was correlated with the *in vivo* bone formation capacity of MBMSCs, CHI3L1 may be an *in vivo* bone formation predictor marker of MBMSCs.

As previously mentioned, human MSCs cultures are composed of a heterogeneous mixture of cells at various stages of differentiation and with distinct osteogenic potentials [24]. Consistent with this report, the MBMSCs used in our experiments showed sample specific variability in the cell growth and osteogenic differentiation. Indeed, the osteogenic differentiation capacity of MBMSCs collected from other parts of the same donor was different (data not shown). Therefore, the differences in osteogenic differentiation capacity *in vitro* and/or bone formation capacity *in vivo* for each MSC are because of differences in the cell composition of the collected MSCs rather than individual differences.

The osteogenic potential of MSCs derived from human iliac crest, femur, and vertebrae declines with aging [25]. The decreased bone formation and fracture repair rate observed with aging is caused by a decrease in the number and/or bone formation capacity of MSCs, and changes in the secretion of cytokines such as interleukin-11 from MSCs [26, 27]. Therefore, the factors secreted from MBMSCs may regulate the osteogenic differentiation of MBMSCs *in vivo*.

CHI3L1, which was identified as an *in vivo* bone formation predictor marker of MBMSCs, is also

known as YKL-40. CHI3L1 is a 39 kDa glycoprotein secreted by various cells such as macrophages, neutrophils, fibroblasts, vascular smooth muscle cells, and endothelial cells [28]. CHI3L1 is involved in normal and tumorigenic angiogenesis [29]. CHI3L1 is also expressed in normal bone marrow and its expression is induced in inflammatory disease and degenerative diseases such as rheumatoid arthritis, asthma, and tumors [28, 30-33]. Multiple myeloma patients with elevated serum CHI3L1 have more severe bone destruction, including increased bone resorption activity and a shorter time to bone disease progression [34]. In a mouse model of osteomyelitis, the inhibition of increased CHI3L1 in the bone marrow resulted in increased expression of proteins involved in Notch signaling and decreased inflammation, resulting in a significant reduction in cortical bone destruction [35]. Alternatively, CHI3L1 secretion is increased by IL-6 induced osteogenic differentiation of human MSCs [36]. CHI3L1 might be act as a negative feedback factor for bone formation. Although several reports have been described for CHI3L1 and bone formation, the effect of increased CHI3L1 on the regeneration of bone with MSCs has not been clarified.

Using real-time RT-PCR and ELISA, we have clarified that MBMSCs synthesized and secreted CHI3L1, and there are large inter-sample and/or sample specific variability in its amount. Although it has been reported that CHI3L1 is not synthesized in undifferentiated iliac MSCs [37], some undifferentiated MBMSCs synthesized and secreted CHI3L1 in this study. MBMSCs have lower chondrogenic and adipogenic differentiation capacity [9] and greater osteogenic differentiation capacity than iliac MSCs [38,

39]. In addition, MBMSCs and iliac MSCs have been reported to have different gene expression according to DNA microarray analysis [40]. Differences in the amount of synthesized CHI3L1 may be because of differences in the inter-sample properties of MBMSCs and iliac MSCs. Comparing the relationship between the CHI3L1 secretion amount and the amount of new bone formation, MBMSCs that secrete a high level of CHI3L1 had low bone formation capacity, and MBMSCs that secrete a low level of CHI3L1 had high bone formation capacity *in vivo*. This result showed that the amount of CHI3L1 secreted into the conditioned medium negatively correlates with the *in vivo* bone formation capacity of the transplanted MBMSCs. We could not find clear correlation between the expression of four proteins (GRO α , MCP-1, MCP-3, and IL-8) and the *in vivo* bone formation capacity of MBMSCs, so they cannot be *in vivo* bone formation predictor markers of MBMSCs.

MBMSC growth and osteogenic differentiation were not affected by CHI3L1. Therefore, the bone formation capacity by MBMSCs themselves would not be affected by secreted CHI3L1 from MBMSCs. Although treatment with CHI3L1 did not affect HUVEC growth, it promoted NHDF growth in a dose dependent manner. Migration of HUVECs and NHDFs were also enhanced by CHI3L1. The effects of CHI3L1 on the growth of NHDFs and migration of HUVECs and NHDFs are consistent with previous reports [41-43]. Furthermore, CHI3L1 infiltrates macrophages and induces the transcription levels of pro-inflammatory cytokines such as IL-6, IL-8, IL-12, IFN- γ , TNF- α , CXCL9, CXCL11, and IL-18 from macrophages, epithelial cells, osteoclasts, and other cells [44]. These pro-inflammatory cytokines

promote fibrosis [45]. In addition, increased IFN- γ suppresses osteoclast differentiation [46] and then the imbalance between bone resorption and bone formation leads to abnormal bone remodeling [47]. CHI3L1 secreted by MBMSC had no effect on MBMSC itself; however, CHI3L1 might have a positive effect on *in situ* vascular endothelial cells and fibroblasts. Indeed, CHI3L1 enhanced the migration of vascular endothelial cells and fibroblasts and promoted angiogenesis and fibroblast growth in our experiments. It is assumed that CHI3L1 released from transplanted MBMSCs induced angiogenesis and fibrosis rather than bone formation.

In the case of low level CHI3L1 secretion into the conditioned medium by undifferentiated MBMSCs, transplanted MBMSCs showed high bone formation *in vivo*. Within the limitations of this study, CHI3L1 could be used as a negative marker to determine the bone formation capacity of MBMSC. However, because CHI3L1 is not the only factor that affects bone formation *in vivo*, it is necessary to consider the other factors that may also be involved in bone formation regulation. Furthermore, to clinically apply CHI3L1 as an *in vivo* bone formation predictor marker of MBMSCs, it is necessary to elucidate the mechanism by which CHI3L1 inhibits bone formation *in vivo*.

5. Conclusions

The results of this study indicate that MBMSCs, which secrete a small amount of CHI3L1 into conditioned medium, showed high *in vivo* bone formation capacity. Conversely, MBMSCs that secreted a large

amount of CHI3L1 into the conditioned medium showed low *in vivo* bone formation capacity. The amount of CHI3L1 in the MBMSC culture conditioned medium might be useful as an *in vivo* bone formation predictor marker of MBMSCs.

Acknowledgments

The authors thank GC for providing the puncture needle; and the patients in Kagoshima University Hospital Special Clinic for Oral Implantology, for the bone marrow samples. This work was supported by Grants-in-Aid for Scientific Research (19K10212, 20H03881) from the Japan Society for the Promotion of Science. We thank Ashleigh Cooper, PhD, from Edanz Group (<https://en-author-services.edanz.com/ac>) for editing a draft of this manuscript.

Figure legends

Fig.1 Characteristics of maxillary/mandibular bone marrow stromal cells (MBMSCs). (A) Cell growth capacity of MBMSCs. Each point shows the cumulative cell number at the time of passage. (B) Osteogenic differentiation potential of MBMSCs. The alkaline phosphatase (ALP) activity was measured on Day 7 after induction of osteogenic differentiation in seven MBMSC samples (mean \pm SD, $n = 3$). (C) Alizarin red staining of MBMSCs. Matrix calcification on Day 14 after induction of osteogenic differentiation was visualized with alizarin red staining.

Fig.2 Bone formation on mice parietal bone with the transplants (MBMSCs, β -TCP, and atelocollagen).

(A) The bottom side of the image shows the orientation of the recipient parietal bone. The transplant site was harvested at 8 weeks for analysis. High-magnification images of hematoxylin-eosin staining show the black boxes in low-magnification.* shows the bone replacement material and the arrows shows newly formed bone. Scale bars: 400 μ m. (B) Bone area/tissue area (BA/TA) ratio (mean \pm SD, $n = 3$).

Fig.3 Antibody arrays of the MBMSC culture supernatant. Protein levels in the supernatant of MBMSC culture determined by antibody-based protein arrays of (A) angiogenesis, (B) chemokine, and (C) cytokines.

Fig.4 Quantification of protein secreted into the supernatant of MBMSC cultures. (A) CHI3L1, (B) GRO α , (C) MCP-1, (D) MCP-3, and (E) IL-8 secretions were examined by ELISA (mean \pm SD, $n = 3$).

Fig.5 Expression of protein genes in MBMSCs. Total RNA was extracted from MBMSCs and the mRNA levels of (A) CHI3L1, (B) GRO α , (C) MCP-1, (D) MCP-3, and (E) IL-8 were determined by quantitative RT-PCR (mean \pm SD, $n = 3$).

Fig.6 Effect of CHI3L1 on cell growth and osteogenic differentiation potential of MBMSCs. (A) MBMSCs were treated with CHI3L1 (0.01–100 ng/ml) or saline for 72 hours, and then a WST-1 assay was performed (mean \pm SD, $n = 3$). (B) The alkaline phosphatase (ALP) activity was measured on Day 7 after induction of osteogenic differentiation with the addition of CHI3L1 (mean \pm SD, $n = 3$). (C) Alizarin red staining of MBMSCs. Matrix calcification on Day 14 after induction of osteogenic differentiation with the addition of CHI3L1 was visualized with alizarin red staining.

Fig.7 Effect of CHI3L1 on human umbilical vein endothelial cells (HUVECs) and normal human dermal fibroblasts (NHDFs).

(A) Cell growth capacity of HUVECs and NHDFs with 0–100 ng/ml of CHI3L1 by the WST-1 assay at 72 hours (mean \pm SD, $n = 3$). (B) Representative photomicrographs of migrating HUVECs treated with CHI3L1 (0.01–100 ng/ml) or saline for 6 hours. (C) Quantitative analysis of the migrating cells is shown (mean \pm SD, $n = 3$). Scale bars: 200 μ m. (D) Representative photomicrographs of migrating NHDFs treated with CHI3L1 (0.01–100 ng/ml) or saline for 6 hours. (E) Quantitative analysis of the migrating cells (mean \pm SD, $n = 3$) * $P < 0.05$, ** $P < 0.01$, *** $P < 0.001$ (VS. 0 ng/mL). Scale bars: 200 μ m.

Fig.8 Histological images of the parietal bone with transplants (MBMSCs, β -TCP, and atelocollagen). The transplant site was harvested at 8 weeks for analysis. (A) Masson's trichrome and (B) CD31

immunostained parietal bone sections of MBMSC1, 3, 5, and 6. High-magnification images of CD31 immunostaining show the black boxes in low-magnification. Scale bars: 400 μm (low-magnification) and 100 μm (High-magnification). (C) Number of running vessels per unit area, excluding recipient bone and β -TCP. Statistical analysis was performed using one-way ANOVA, and Tukey's post hoc correction was applied (mean \pm SD, $n = 3$). * $P < 0.05$.

References

1. Younger EM, Chapman MW. Morbidity at bone graft donor sites. *J Orthop Trauma*. 1989;3(3):192-5.
2. Caplan AI, Bruder SP. Mesenchymal stem cells: building blocks for molecular medicine in the 21st century. *Trends Mol Med*. 2001 Jun;7(6):259-64.
3. Deans RJ, Moseley AB. Mesenchymal stem cells: biology and potential clinical uses. *Exp Hematol*. 2000 Aug;28(8):875-84.
4. Friedenstein AJ, Piatetzky-Shapiro II, Petrakova KV. Osteogenesis in transplants of bone marrow cells. *J Embryol Exp Morphol*. 1966 Dec;16(3):381-90.
5. Pittenger MF, Mackay AM, Beck SC, Jaiswal RK, Douglas R, Mosca JD, *et al*. Multilineage potential of adult human mesenchymal stem cells. *Science*. 1999 Apr 2;284(5411):143-7.
6. Risbud MV, Shapiro IM, Guttapalli A, Di Martino A, Danielson KG, Beiner JM, *et al*. Osteogenic potential of adult human stem cells of the lumbar vertebral body and the iliac crest. *Spine (Phila Pa 1976)*. 2006 Jan 1;31(1):83-9.
7. Jaiswal N, Haynesworth SE, Caplan AI, Bruder SP. Osteogenic differentiation of purified, culture-expanded human mesenchymal stem cells in vitro. *J Cell Biochem*. 1997 Feb;64(2):295-312.
8. Igarashi A, Segoshi K, Sakai Y, Pan H, Kanawa M, Higashi Y, *et al*. Selection of common markers for bone marrow stromal cells from various bones using real-time RT-PCR: effects of passage number and donor age. *Tissue Eng*. 2007 Oct;13(10):2405-17.
9. Matsubara T, Suardita K, Ishii M, Sugiyama M, Igarashi A, Oda R, *et al*. Alveolar bone marrow as a cell source for regenerative medicine: differences between alveolar and iliac bone marrow stromal cells. *J Bone Miner Res*. 2005 Mar;20(3):399-409.

10. Egusa H, Sonoyama W, Nishimura M, Atsuta I, Akiyama K. Stem cells in dentistry--part I: stem cell sources. *J Prosthodont Res.* 2012 Jul;56(3):151-65.
11. Gan L, Liu Y, Cui D, Pan Y, Zheng L, Wan M. Dental Tissue-Derived Human Mesenchymal Stem Cells and Their Potential in Therapeutic Application. *Stem Cells Int.* 2020 Sep 1;2020:8864572.
12. Wang X, Xing H, Zhang G, Wu X, Zou X, Feng L, *et al.* Restoration of a Critical Mandibular Bone Defect Using Human Alveolar Bone-Derived Stem Cells and Porous Nano-HA/Collagen/PLA Scaffold. *Stem Cells Int.* 2016;2016:8741641.
13. Pevsner-Fischer M, Levin S, Zipori D. The origins of mesenchymal stromal cell heterogeneity. *Stem Cell Rev Rep.* 2011 Sep;7(3):560-8.
14. Granéli C, Thorfve A, Ruetschi U, Brisby H, Thomsen P, Lindahl A, Karlsson C. Novel markers of osteogenic and adipogenic differentiation of human bone marrow stromal cells identified using a quantitative proteomics approach. *Stem Cell Res.* 2014 Jan;12(1):153-65.
15. Marom R, Shur I, Solomon R, Benayahu D. Characterization of adhesion and differentiation markers of osteogenic marrow stromal cells. *J Cell Physiol.* 2005 Jan;202(1):41-8.
16. Prins HJ, Braat AK, Gawlitta D, Dhert WJ, Egan DA, Tijssen-Slump E, *et al.* In vitro induction of alkaline phosphatase levels predicts in vivo bone forming capacity of human bone marrow stromal cells. *Stem Cell Res.* 2014 Mar;12(2):428-40.
17. Davies OG, Cooper PR, Shelton RM, Smith AJ, Scheven BA. Isolation of adipose and bone marrow mesenchymal stem cells using CD29 and CD90 modifies their capacity for osteogenic and adipogenic differentiation. *J Tissue Eng.* 2015 Jun 23;6:2041731415592356.
18. Yamamoto M, Nakata H, Hao J, Chou J, Kasugai S, Kuroda S. Osteogenic Potential of Mouse Adipose-Derived Stem Cells Sorted for CD90 and CD105 In Vitro. *Stem Cells Int.* 2014;2014:576358.
19. Park YT, Lee SM, Kou X, Karabucak B. The Role of Interleukin 6 in Osteogenic and Neurogenic Differentiation Potentials of Dental Pulp Stem Cells. *J Endod.* 2019 Nov;45(11):1342-1348.
20. Bian S, Zhang L, Duan L, Wang X, Min Y, Yu H. Extracellular vesicles derived from human bone marrow mesenchymal stem cells promote angiogenesis in a rat myocardial infarction model. *J Mol Med (Berl).* 2014 Apr;92(4):387-97.
21. Oslugi M, Katagiri W, Yoshimi R, Inukai T, Hibi H, Ueda M. Conditioned media from mesenchymal stem cells enhanced bone regeneration in rat calvarial bone defects. *Tissue Eng Part A.* 2012 Jul;18(13-14):1479-89.
22. Suehiro F, Ishii M, Asahina I, Murata H, Nishimura M. Low-serum culture with novel medium promotes maxillary/mandibular bone marrow stromal cell proliferation and osteogenic differentiation ability. *Clin Oral Investig.* 2017 Dec;21(9):2709-2719.

23. Dominici M, Le Blanc K, Mueller I, Slaper-Cortenbach I, Marini F, Krause D, *et al.* Minimal criteria for defining multipotent mesenchymal stromal cells. The International Society for Cellular Therapy position statement. *Cytotherapy*. 2006;8(4):315-7.
24. Phinney DG, Kopen G, Righter W, Webster S, Tremain N, Prockop DJ. Donor variation in the growth properties and osteogenic potential of human marrow stromal cells. *J Cell Biochem*. 1999 Dec 1;75(3):424-36.
25. Wang X, Zou X, Zhao J, Wu X, E L, Feng L, *et al.* Site-Specific Characteristics of Bone Marrow Mesenchymal Stromal Cells Modify the Effect of Aging on the Skeleton. *Rejuvenation Res*. 2016 Oct;19(5):351-361.
26. Cheleuitte D, Mizuno S, Glowacki J. In vitro secretion of cytokines by human bone marrow: effects of age and estrogen status. *J Clin Endocrinol Metab*. 1998 Jun;83(6):2043-51.
27. Rosen CJ, Verault D, Steffens C, Cheleuitte D, Glowacki J. Effects of age and estrogen status on the skeletal IGF regulatory system. Studies with human marrow. *Endocrine*. 1997 Aug;7(1):77-80.
28. Libreros S, Iragavarapu-Charyulu V. YKL-40/CHI3L1 drives inflammation on the road of tumor progression. *J Leukoc Biol*. 2015 Dec;98(6):931-6.
29. Shao R, Hamel K, Petersen L, Cao QJ, Arenas RB, Bigelow C, *et al.* YKL-40, a secreted glycoprotein, promotes tumor angiogenesis. *Oncogene*. 2009 Dec 17;28(50):4456-68.
30. Kawada M, Seno H, Kanda K, Nakanishi Y, Akitake R, Komekado H, *et al.* Chitinase 3-like 1 promotes macrophage recruitment and angiogenesis in colorectal cancer. *Oncogene*. 2012 Jun 28;31(26):3111-23.
31. Ling H, Recklies AD. The chitinase 3-like protein human cartilage glycoprotein 39 inhibits cellular responses to the inflammatory cytokines interleukin-1 and tumour necrosis factor-alpha. *Biochem J*. 2004 Jun 15;380(Pt 3):651-9.
32. Ober C, Tan Z, Sun Y, Possick JD, Pan L, Nicolae R, *et al.* Effect of variation in CHI3L1 on serum YKL-40 level, risk of asthma, and lung function. *N Engl J Med*. 2008 Apr 17;358(16):1682-91.
33. Recklies AD, Ling H, White C, Bernier SM. Inflammatory cytokines induce production of CHI3L1 by articular chondrocytes. *J Biol Chem*. 2005 Dec 16;280(50):41213-21.
34. Mylin AK, Abildgaard N, Johansen JS, Andersen NF, Heckendorff L, Standal T, *et al.* High serum YKL-40 concentration is associated with severe bone disease in newly diagnosed multiple myeloma patients. *Eur J Haematol*. 2008 Apr;80(4):310-7.
35. Chen X, Jiao J, He X, Zhang J, Wang H, Xu Y, *et al.* CHI3L1 regulation of inflammation and the effects on osteogenesis in a *Staphylococcus aureus*-induced murine model of osteomyelitis. *FEBS J*. 2017 Jun;284(11):1738-1747.
36. Lieder R, Sigurjonsson OE. The Effect of Recombinant Human Interleukin-6 on Osteogenic

- Differentiation and YKL-40 Expression in Human, Bone Marrow-Derived Mesenchymal Stem Cells. *Biores Open Access*. 2014 Feb 1;3(1):29-34.
37. Hoover DJ, Zhu V, Chen R, Briley K Jr, Rameshwar P, Cohen S, *et al*. Expression of the chitinase family glycoprotein YKL-40 in undifferentiated, differentiated and trans-differentiated mesenchymal stem cells. *PLoS One*. 2013 May 9;8(5):e62491.
 38. Akintoye SO, Lam T, Shi S, Brahim J, Collins MT, Robey PG. Skeletal site-specific characterization of orofacial and iliac crest human bone marrow stromal cells in same individuals. *Bone*. 2006 Jun;38(6):758-68.
 39. Liu Y, Wang H, Dou H, Tian B, Li L, Jin L, *et al*. Bone regeneration capacities of alveolar bone mesenchymal stem cells sheet in rabbit calvarial bone defect. *J Tissue Eng*. 2020 Jun 10;11:2041731420930379.
 40. Lee JT, Choi SY, Kim HL, Kim JY, Lee HJ, Kwon TG. Comparison of gene expression between mandibular and iliac bone-derived cells. *Clin Oral Investig*. 2015 Jul;19(6):1223-33.
 41. Recklies AD, White C, Ling H. The chitinase 3-like protein human cartilage glycoprotein 39 (HC-gp39) stimulates proliferation of human connective-tissue cells and activates both extracellular signal-regulated kinase- and protein kinase B-mediated signalling pathways. *Biochem J*. 2002 Jul 1;365(Pt 1):119-26.
 42. Malinda KM, Ponce L, Kleinman HK, Shackelton LM, Millis AJ. Gp38k, a protein synthesized by vascular smooth muscle cells, stimulates directional migration of human umbilical vein endothelial cells. *Exp Cell Res*. 1999 Jul 10;250(1):168-73.
 43. Park SJ, Jun YJ, Kim TH, Jung JY, Hwang GH, Jung KJ, *et al*. Increased expression of YKL-40 in mild and moderate/severe persistent allergic rhinitis and its possible contribution to remodeling of nasal mucosa. *Am J Rhinol Allergy*. 2013 Sep-Oct;27(5):372-80.
 44. Yeo IJ, Lee CK, Han SB, Yun J, Hong JT. Roles of chitinase 3-like 1 in the development of cancer, neurodegenerative diseases, and inflammatory diseases. *Pharmacol Ther*. 2019 Nov;203:107394.
 45. Wynn TA, Vannella KM. Macrophages in Tissue Repair, Regeneration, and Fibrosis. *Immunity*. 2016 Mar 15;44(3):450-462.
 46. Takayanagi H, Ogasawara K, Hida S, Chiba T, Murata S, Sato K, *et al*. T-cell-mediated regulation of osteoclastogenesis by signalling cross-talk between RANKL and IFN-gamma. *Nature*. 2000 Nov 30;408(6812):600-5.
 47. Feng X, McDonald JM. Disorders of bone remodeling. *Annu Rev Pathol*. 2011;6:121-45.

Gene		Sequence (5'-3')
CHI3L1	Forward	GTGAGGCATCGCAATGTAAGAC
	Reverse	AAATTCCTTGCCAGGCTTG
GRO α	Forward	AGCTTGCCTCAATCCTGCAT
	Reverse	GCACATACATTCCCCTGCCT
MCP-1	Forward	GCTCATAGCAGCCACCTTCA
	Reverse	TCCCAGGGGTAGAACTGTGG
MCP-3	Forward	ATGAAAGCCTCTGCAGCACT
	Reverse	AGGTAGAGAAGGGAGGAGCA
IL-8	Forward	TCTGTCTGGACCCCAAGGAA
	Reverse	GCAACCCTACAACAGACCCA
GAPDH	Forward	CGACCACTTTGTCAAGCTCA
	Reverse	AGGGGAGATTCAGTGTGGTG

Table 1. Nucleotide sequences of primers used for real-time RT PCR

	CD73	CD90	CD105	CD14	CD34	CD45
MBMSC1	99.90	99.95	99.20	0.10	0.15	0.30
MBMSC2	99.78	99.95	99.85	0.30	0.35	0.50
MBMSC3	99.50	99.60	99.80	3.40	0	0.15
MBMSC4	99.75	99.60	99.45	0.15	0.10	0.30
MBMSC5	99.90	99.85	99.85	3.65	0.10	0.10
MBMSC6	99.95	100	99.55	1.05	0.15	0.25
MBMSC7	100	100	99.35	1.10	0.10	0.15

Table 2. Expression rates of cell surface antigens in maxillary/mandibular bone marrow stromal cells (MBMSCs). Seven MBMSC harvests were analyzed by flow cytometry to investigate the expression profiles of cell surface antigens. High expression of CD73, CD90, and CD105 indicates MBMSC positive, and low/no expression of CD14, CD34, CD45 indicates MBMSC negative. The number shows the positive rate.

	Expression level of CHI3L1 (pg/ml/10000 cells)	BA/TA (%)
MBMSC1	249 ± 18.6	0.24 ± 0.09
MBMSC2	829 ± 148.1	1.84 ± 0.15
MBMSC3	11 ± 25.0	35.2 ± 5.48
MBMSC4	0.09 ± 4.0	14.12 ± 1.24
MBMSC5	35 ± 8.6	25.69 ± 1.74
MBMSC6	646 ± 115.0	1.21 ± 0.24
MBMSC7	0.02 ± 0.0	23.62 ± 2.10

Table 3. Bone area/tissue area (BA/TA) ratios and CHI3L1 secretion.

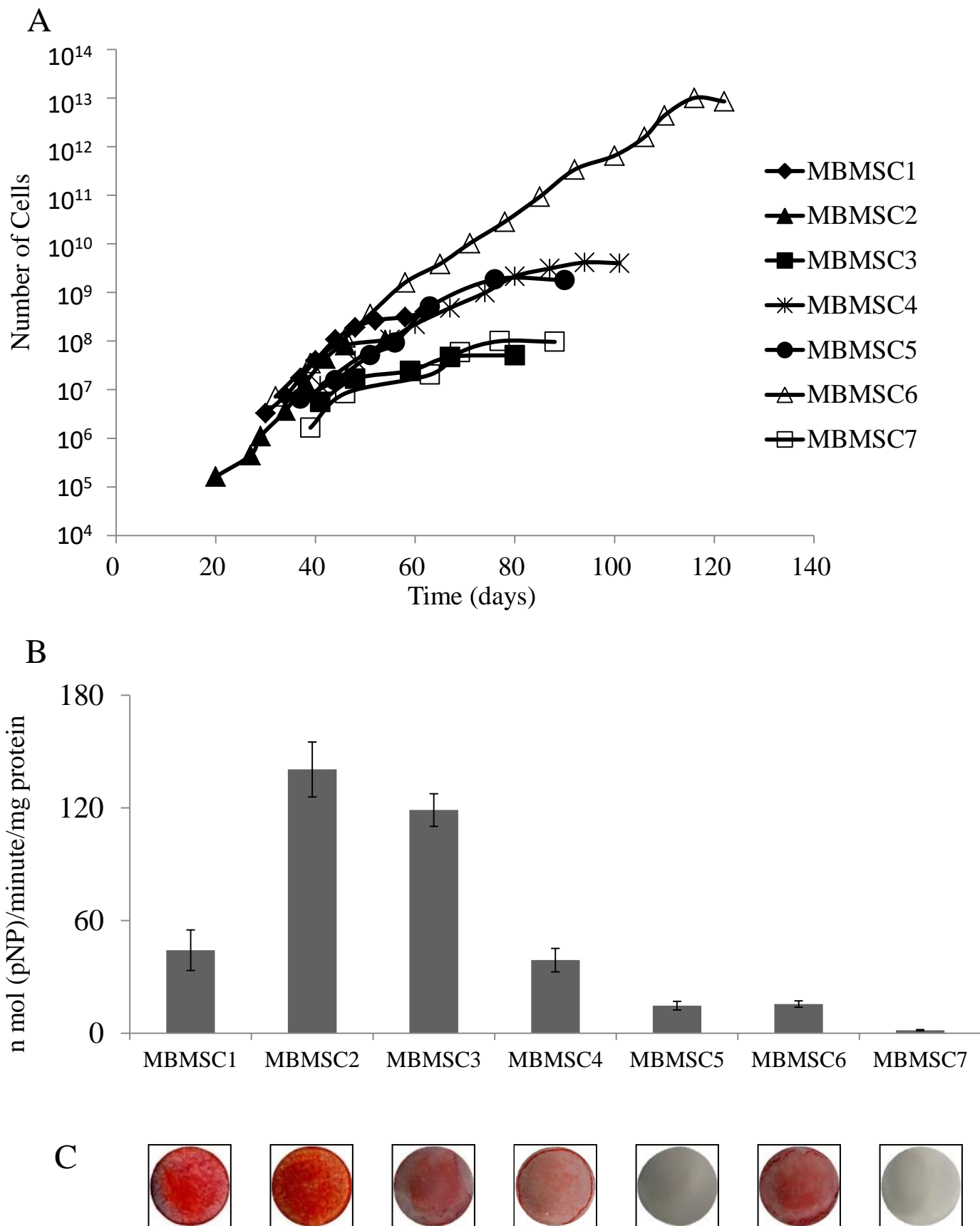


Fig. 1

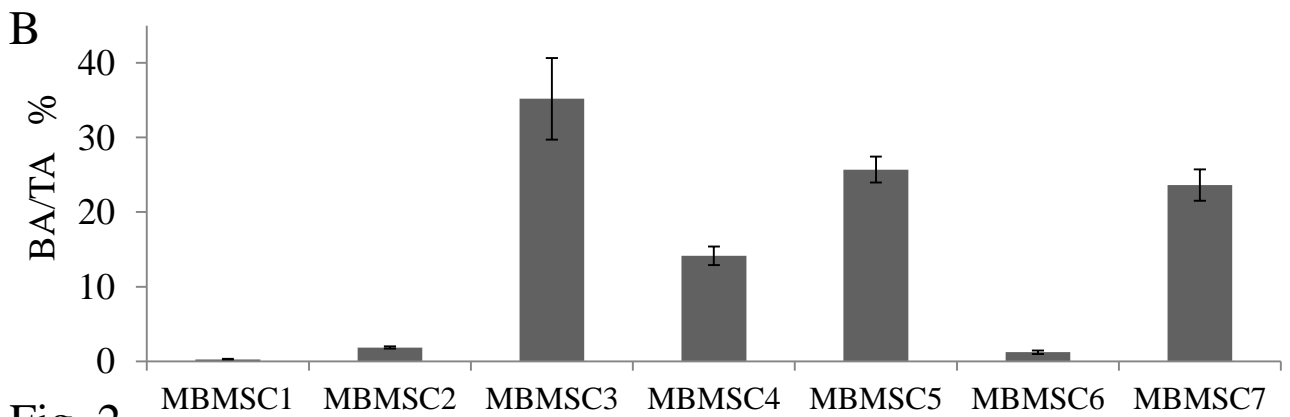
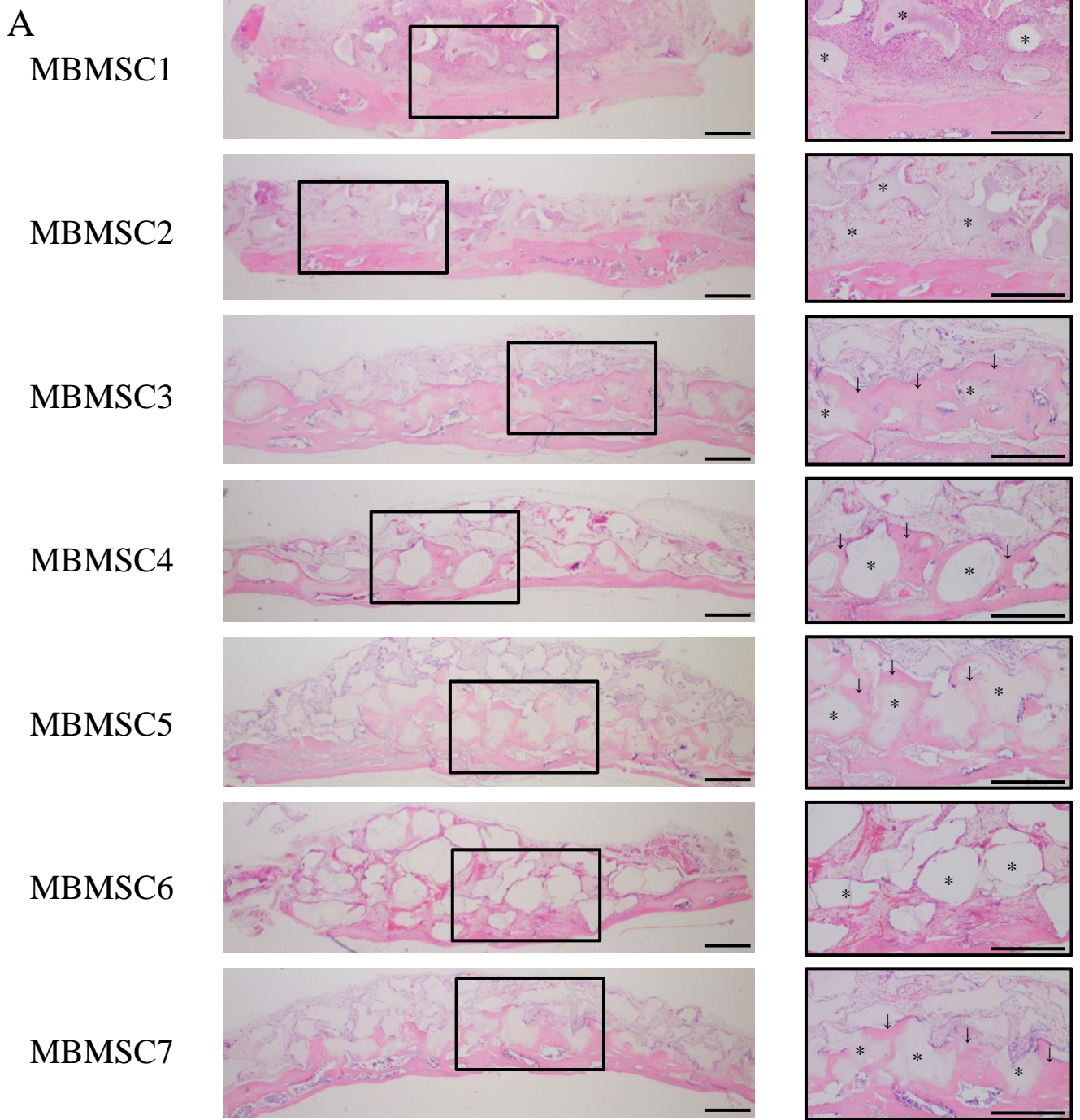


Fig. 2

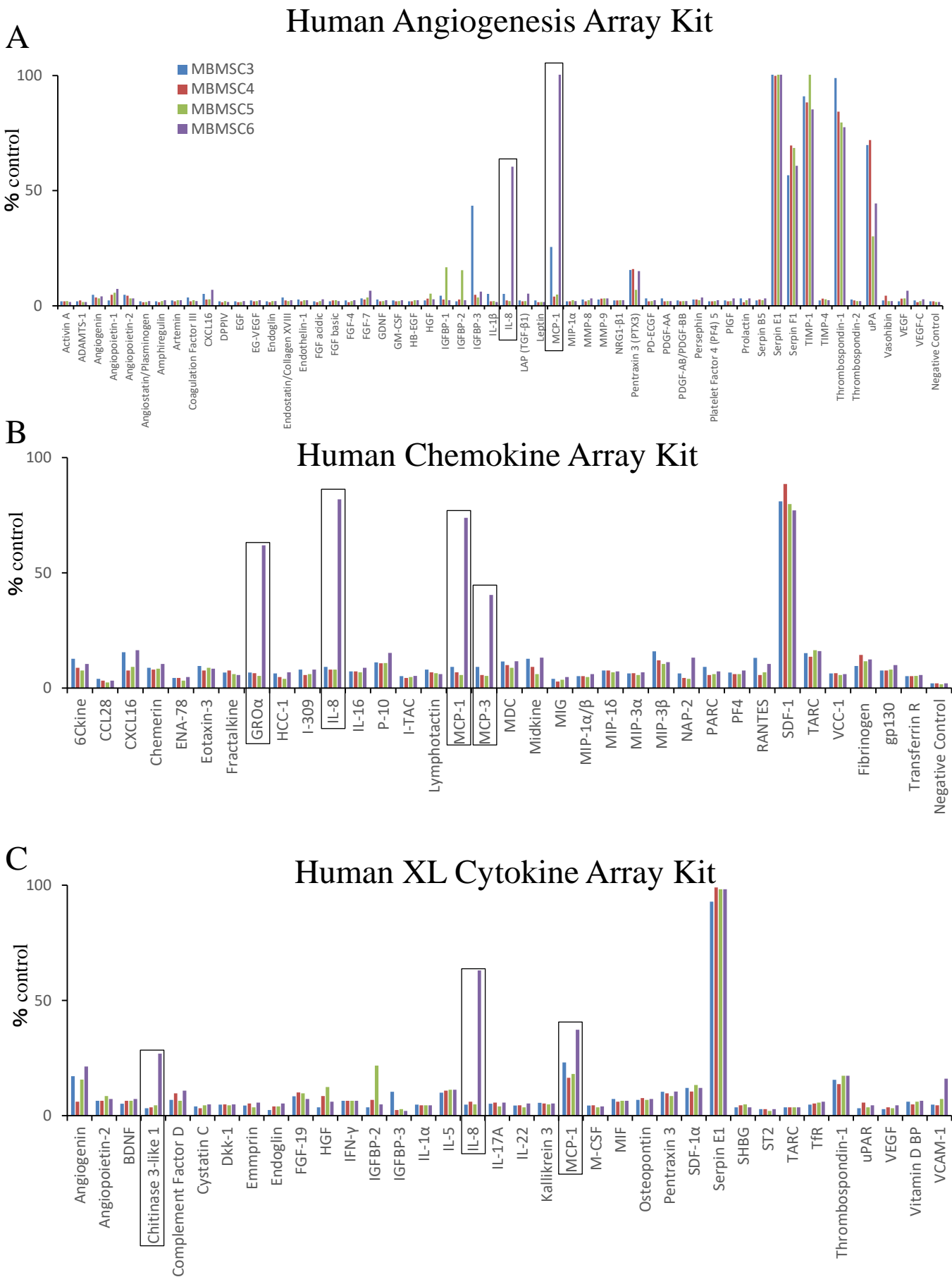


Fig. 3

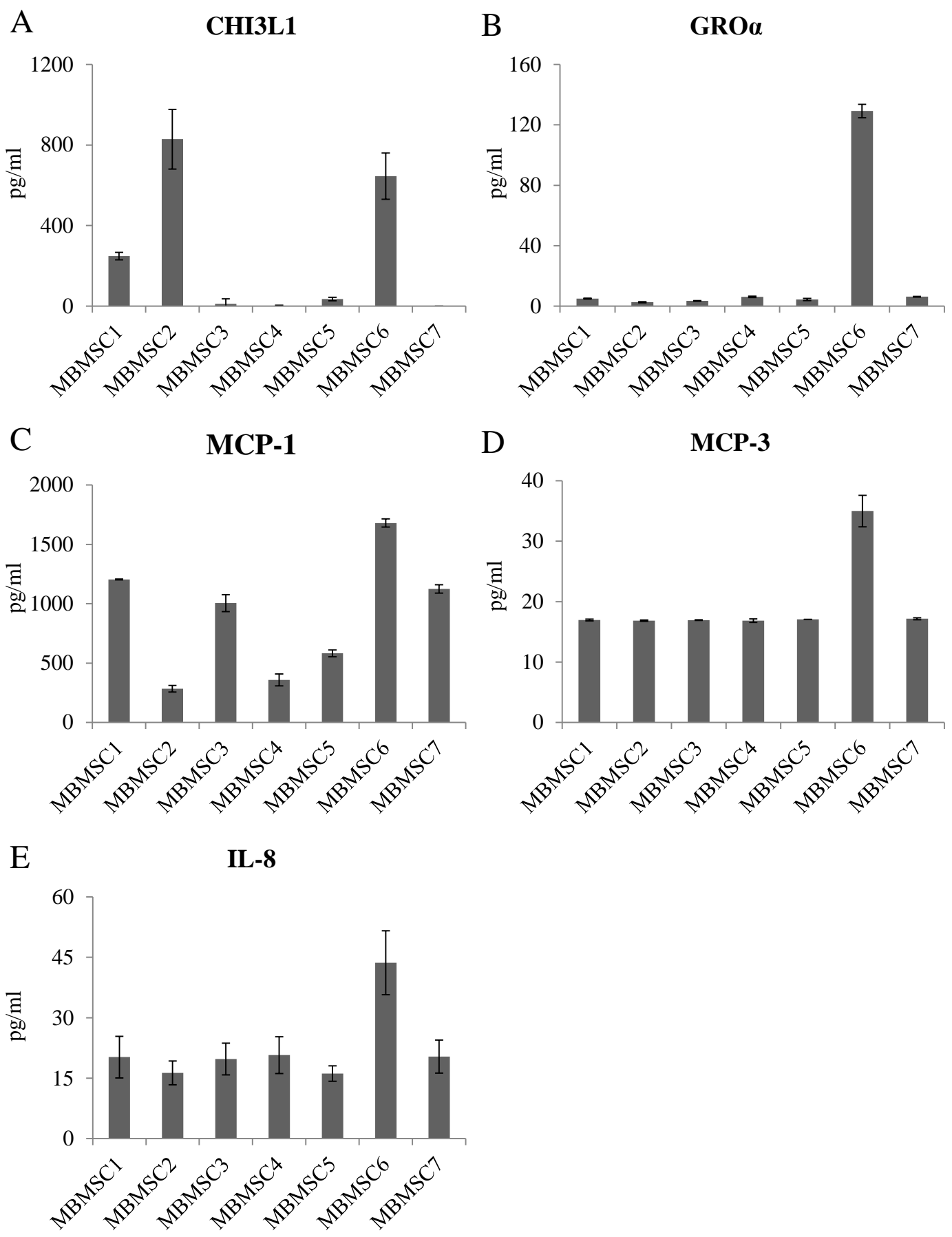


Fig.4

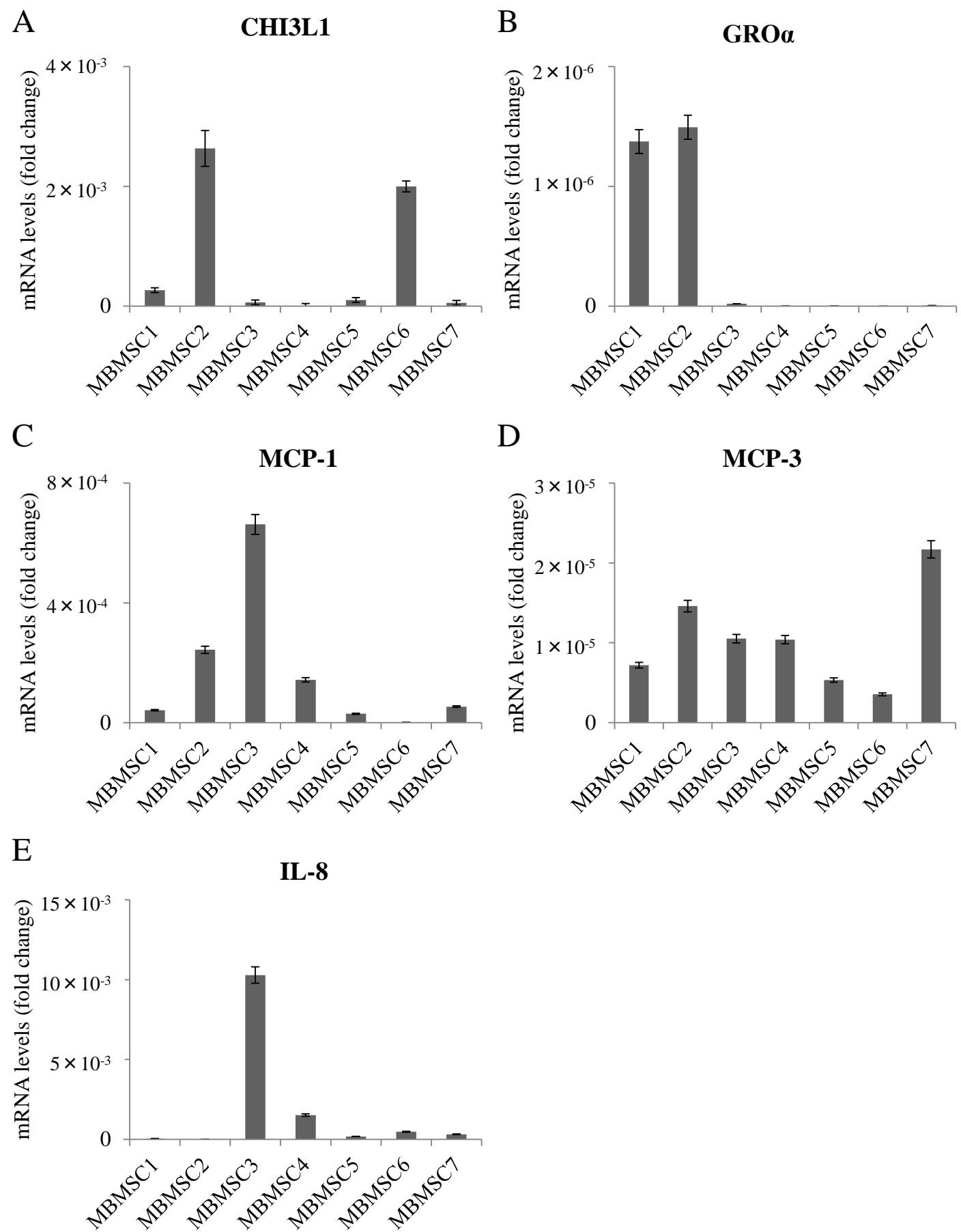
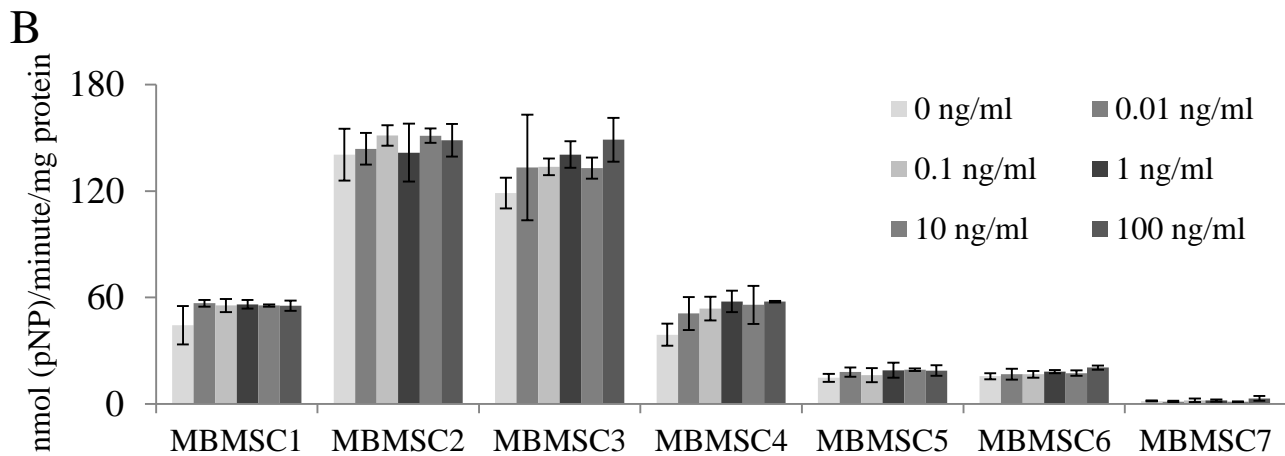
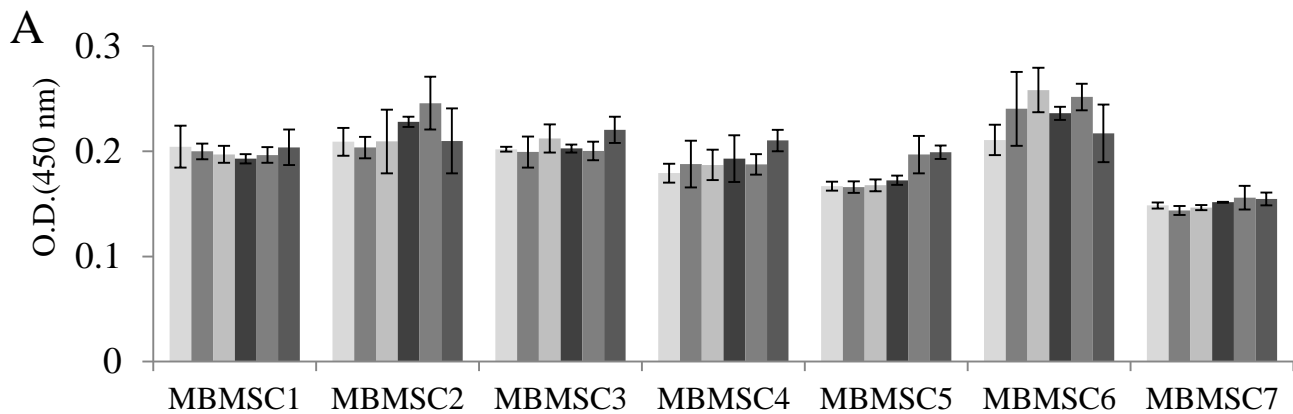


Fig. 5



C

	CHI3L1 (ng/ml)					
	0	0.01	0.1	1	10	100
MBMSC1						
MBMSC2						
MBMSC3						
MBMSC4						
MBMSC5						
MBMSC6						
MBMSC7						

Fig. 6

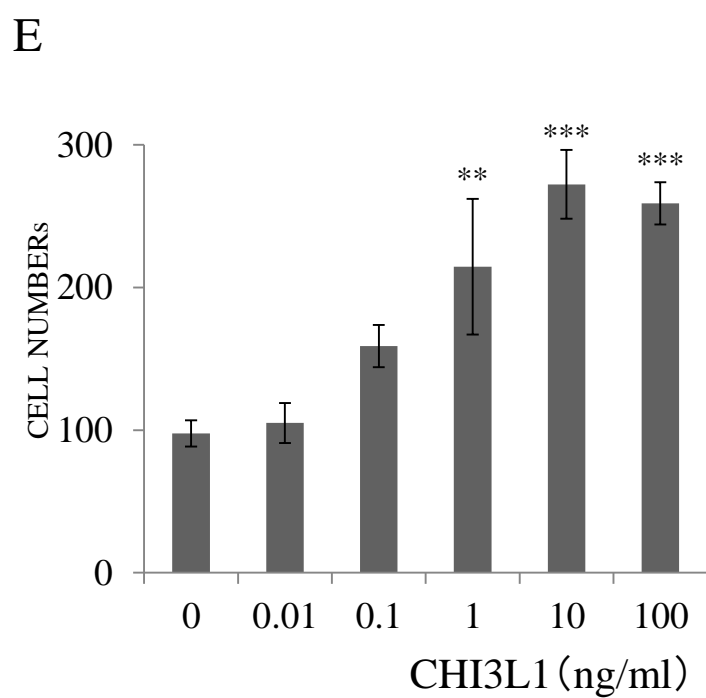
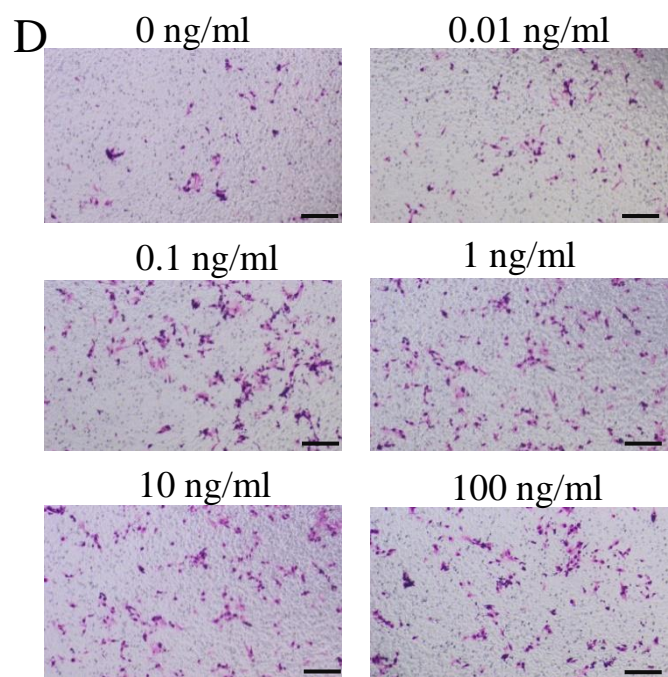
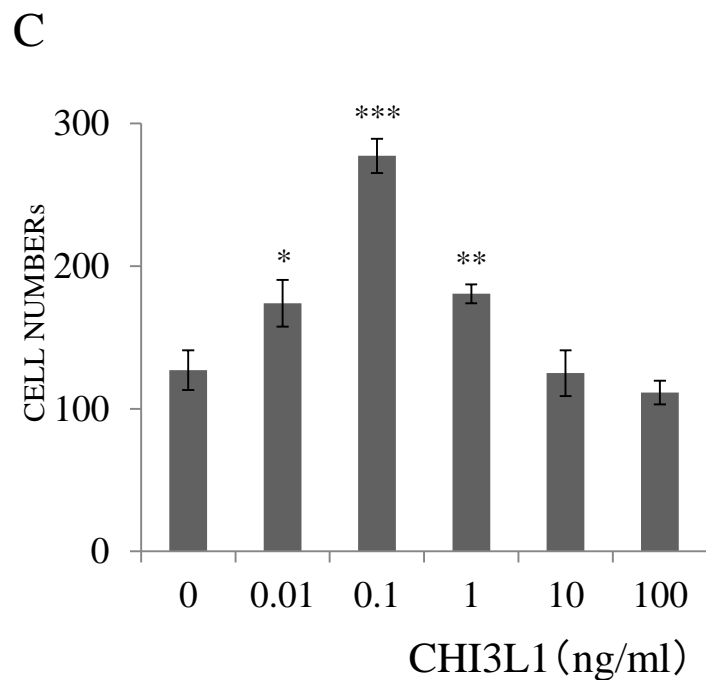
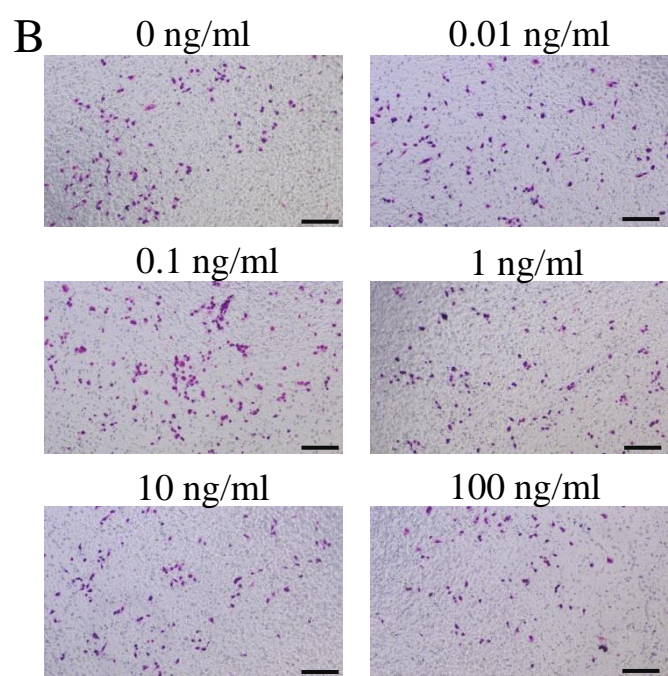
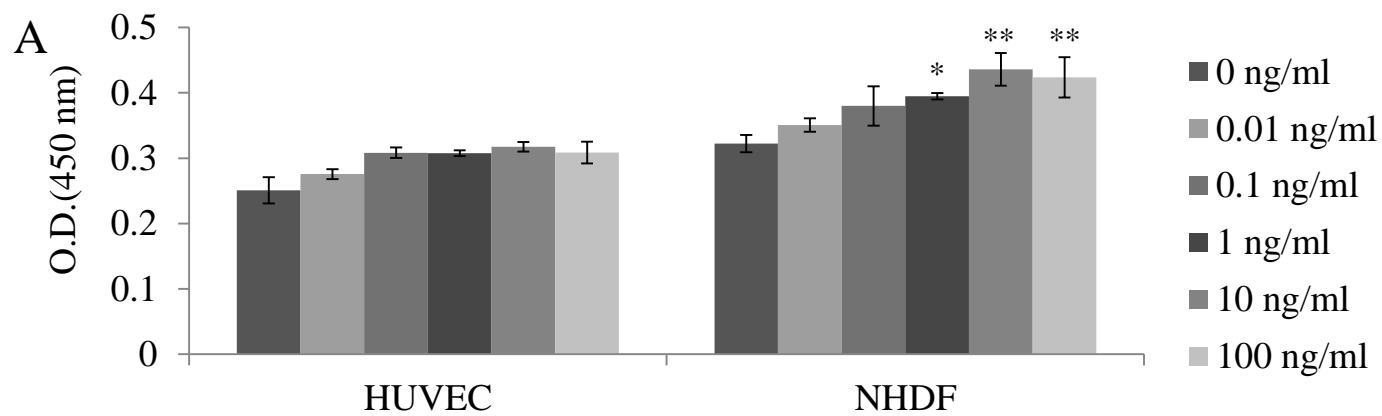


Fig. 7

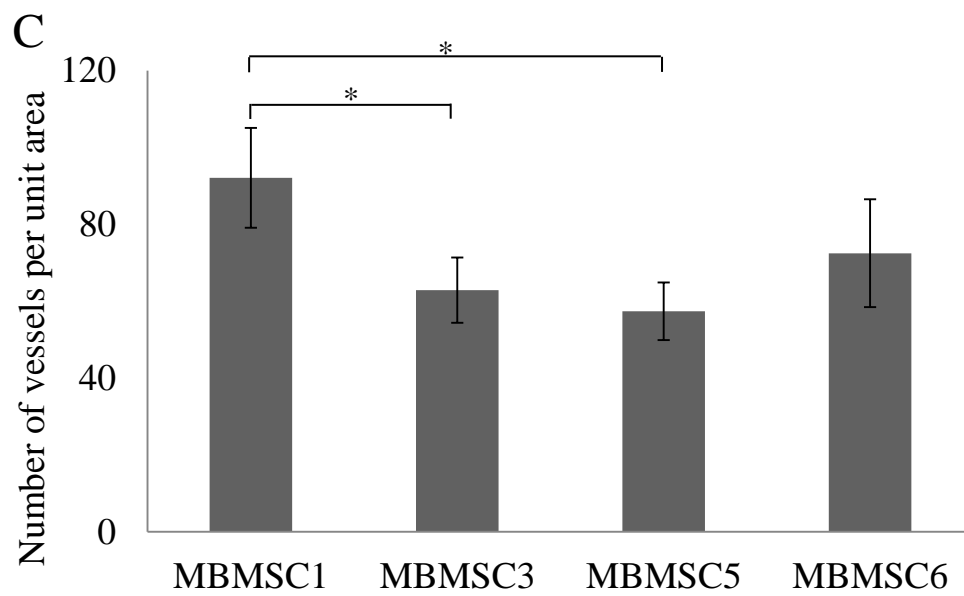
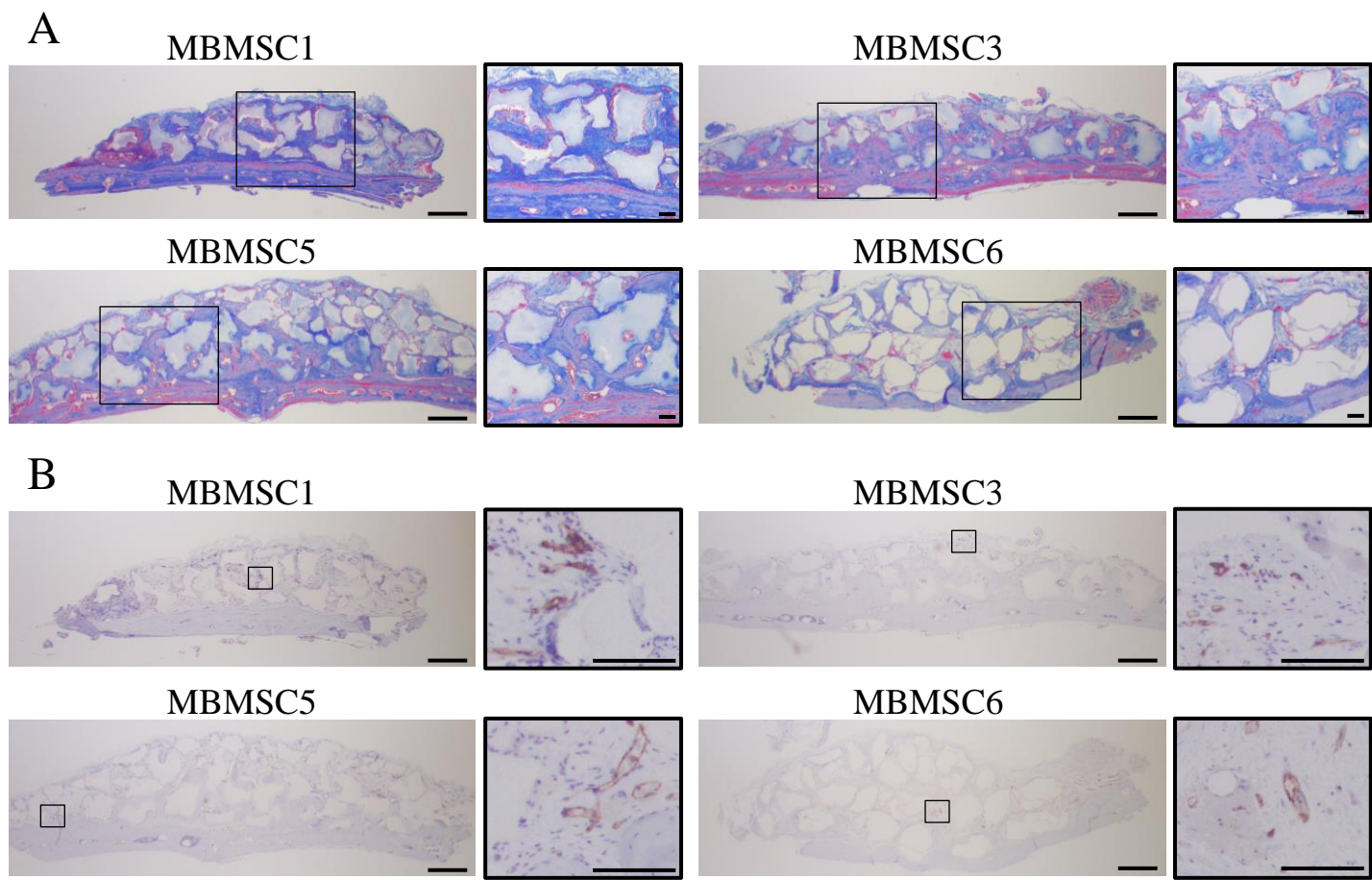


Fig. 8